Desalination and Water Treatment
www.deswater.com

17 (2010) 72–79
May

1944-3994/1944-3986
doi: 10.5004/dwt.2010.1701

Carbon nanotube based composite membranes for water desalination by membrane distillation

Ludovic Dumée[a,b*], Kallista Sears[a*], Jürg Schütz[a], Niall Finn[a], Mikel Duke[b], Stephen Gray[b]

[a]*CSIRO Materials Science and Engineering, Bayview Ave, Clayton Vic 3168, Australia*
[b]*Victoria University Werribee Campus, Hoppers Lane, Werribee PO Box 14428 Melbourne, Victoria, 8001, Australia*
Tel: +61 (0)3 9545 2107; Fax: +61 (0)3 9545 2363
Email: ludovic.dumee@csiro.au and kallista.sears@csiro.au

Received 3 August 2009; accepted 23 November 2009

ABSTRACT

New technologies are required to improve desalination efficiency and increase water treatment capacities. One promising low energy technique to produce potable water from either sea or sewage water is membrane distillation (MD). However, to be competitive with other desalination processes, membranes need to be designed specifically for the MD process requirements. Here we report on the design of carbon nanotube (CNT) based composite material membranes for direct contact membrane distillation (DCMD). The membranes were characterized and tested in a DCMD setup under different feed temperatures and test conditions. The composite CNT structures showed significantly improved performance compared to their pure self-supporting CNT counterparts. The best composite CNT membranes gave permeabilities as high as 3.3×10^{-12} kg/(m × s × Pa) with an average salt rejection of 95% and lifespan of up to 39 h of continuous testing, making them highly promising candidates for DCMD.

Keywords: Desalination; Nanotube; Bucky-paper; Composite material; Membrane distillation

1. Introduction

Carbon nanotube (CNT) [1] based membranes have attracted interest over the past eight years. Several groups have reported on CNT composite material membranes for applications such as pervapouration of cyclohexane/benzene [2], nanofiltration [3,4] and separation of hydrocarbons [5]. However to our knowledge no other group has reported on CNT based membranes for use in membrane distillation (MD). MD is an alternative technique for the purification of sea or sewage water. In a direct contact membrane distillation (DCMD) setup a hydrophobic membrane acts as a barrier between a warm feed (e.g. sea water) and a cold permeate of fresh water. A difference in water vapour pressure is generated due to the temperature gradient across the membrane and leads to water vapour transfer from the hot to the cold side. The water vapour condenses on the cold side creating fresh water as illustrated in Fig. 1 [6–8].

Current MD processes typically use PVDF or PTFE membranes. While these membranes are highly hydrophobic and exhibit reasonable porosity (~75%), they are difficult to process and expensive. For MD to compete with the other more established desalination techniques, such as reverse osmosis, it is important that new membranes structures are developed specifically suited to the MD process.

*Corresponding authors

Presented at the Fifth Conference of the Aseanian Membrane Society Aseania 2009 "Recent Progress in Membrane Science and Technology", 12–14 July 2009, Kobe, Japan.

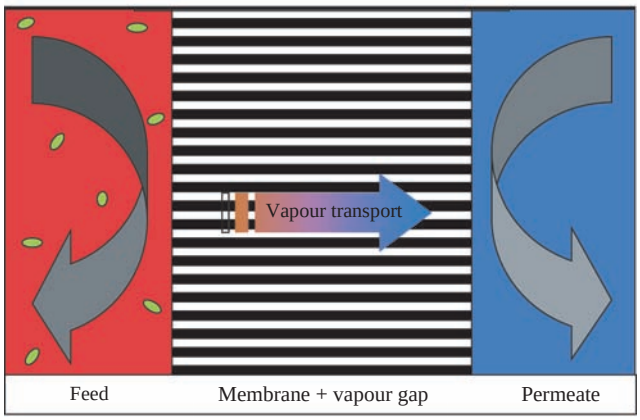

Fig. 1. DCMD concept.

One promising structure is the CNT bucky-paper (BP), a non-woven structure of randomly orientated CNTs. Self-supporting BPs were characterized by us in a previous study [9] and found to exhibit many properties desirable for DCMD [7]. Most importantly, they exhibited a high porosity ($\sim$90%) and contact angle with deionised water ($\sim$120°), a thermal conductivity of $\sim$2.3 W/m × K and a tensile Young's modulus of $\sim$1 GPa. Both scanning electron microscope (SEM) analysis and particle exclusion tests gave an average pore size of $\sim$25 nm, and BET tests indicated a high specific surface area of $\sim$200 m^2/g, comparable to those reported in the literature [10]. Furthermore other studies have shown that they are chemically stable in seawater [11].

We previously demonstrated that the self-supporting CNT BP membranes, a non-woven structure of entangled CNTs, can be used to desalinate synthetic seawater via the DCMD process [9]. These membranes showed lifespans of up to 3 h under continuous operation. Their permeability was calculated to be $\sim 0.8 \times 10^{-12}$ kg m^{-1} s^{-1} Pa^{-1} and their salt rejection efficiency was typically greater than 88%. However, ageing of the membranes over time limited their performance and reinforced membranes need to be designed.

In this work several types of composite CNT structures were processed from self-supporting CNT BPs to improve their lifetime and performance. These composite structures aimed to exploit the desirable CNT BP properties, while also incorporating polymeric materials to improve their strength. The composite structures were characterized with various techniques such as SEM, contact angle measurements and BET surface area analysis, and were also tested in a DCMD setup.

2. Experimental details

2.1. CNT growth

The multiwalled CNTs (9–10 walls) were grown by chemical vapour deposition at CSIRO Material Science and Engineering, Melbourne Australia. A 5 nm thick iron catalyst film was deposited onto a silicon substrate bearing a thin silicon dioxide layer. A mixture of helium (95%)–acetylene (5%) was used as the carbon feedstock and heated to between 650°C and 750°C. The CNTs typically have an outer diameter of $\sim$10–15 nm and length of 150–300 μm [12].

2.2. CNT BP composite membrane fabrication

First, as grown CNTs were first dispersed in propan-2-ol. The suspensions were sonicated, up to five times, for 15 min and at 150 W, in a sonicating bath. Once a well-dispersed CNT suspension was achieved, it was immediately filtered through a Millipore filtration unit. During this process the CNTs were captured on a poly(ethersulfone) (PES) membrane (0.22 μm pore size, Millipore) to produce a pure self-supporting CNT BP.

Composite CNT BP membranes were produced by three methods. The first method involved hot pressing self-supporting BPs between two layers of $\sim$55% porous poly(propylene) (PP) supports. The three layers were maintained between two stainless steel plates and hot-pressed at 36.9 kN for 15 min at 80°C. This structure is referred to throughout the text as the ''sandwiched BP'' composite.

The second structure was a slight variation of the first and referred to as the ''filtered sandwiched BP'' composite. Suspensions of dispersed CNTs were filtered through a PP support (with a PES membrane underneath). In this case the CNTs were collected on and within the pores of the PP support. The PP-CNT cake was sandwiched with another layer of PP support and hot-pressed under the same conditions given above.

Thirdly, a number of ''polymer infiltrated BP'' membranes were formed by vacuum filtration of a 5% polymer/solvent solution through the self-supporting BP. Solutions of either poly(styrene) (PS) or poly(vinyldifluoride) (PVDF) in dimethylformamide (DMF) were used. After polymer infiltration, analytical grade DMF was filtered through the membrane to backwash the membrane and remove any non-bonded polymer.

Poly(tetrafluroethylene) (PTFE) membranes, (0.22 micron nominal pore size, Millipore) were also characterized and tested as control membranes.

2.3. Membrane characterization

SEM was used to examine the surface structure of the composite BP membranes and was performed with a Philips FEG SEM at 2 kV and 7.5 mm working distance. An FEI Nova nanolab 200 Dual Beam Focused Ion Beam (FIB) was used to form cross sections of the composite CNT BP membranes. Milling was performed with a 1 nA, 30 kV Ga ion beam, followed by 0.3 nA cleaning steps. Contact angles were measured with a 2 mL pycnometer as described [13]. An average BET surface area was determined by N2 adsorption on a Micromeretics Tristar 3000 [14]. The samples were first degassed for 70 h and then analyzed at 77 K. Finally, a pocket goniometer PG-3 from Fibro Systems was used to determine contact angles. The tests were performed at 20°C with 4 μL drops of deionised water [15]. The characterization techniques and conditions used are described in more detail in a previous study [9].

2.4. DCMD setup

For DCMD testing the membranes were placed inside a sealed PTFE module. A peristaltic pump fitted with two coupled heads was used to control both permeate and feed flow rates, which were kept constant at 300 mL/min. The temperatures of the water streams were also kept constant and no significant temperature drop measured between the inlet and the outlet of the module. The temperature was therefore considered constant over the membrane area. The membrane test area was a 25.4 mm diameter disc. Electrical conductivity and temperature of the hot and cold electrolytes, as well as water level transferred to the cold side, were monitored over time. Tests were performed with deionised water and synthetic seawater (35 g/L NaCl solutions at 11 mS/cm).

Each membrane was tested at six different feed temperatures (20°C; 35°C; 50°C; 65°C; 80°C and 95°C) while the cold permeate was kept constant at 5°C. Partial pressure differences were calculated for each set of temperatures using Antoine's equation:

$$P = \mathrm{e}^{\left(23.328-\frac{3841}{T-45}\right)}, \quad (1)$$

where the water vapour partial pressure P is in Pa and the temperature T in Kelvin (K).

3. Results

3.1. Membrane characterization

The ''sandwiched BP'' composite structures were expected to exhibit similar properties to the self-supporting BPs. The primary effect of the PP support layers was to reduce the BP surface area exposed to both permeate and feed streams. The porosity of the support was measured to be ~55% (Fig. 2). The support macro pores were ovals with major and minor axes of 750 and 300 μm, respectively. The process of hot pressing may have also slightly compacted the BP structure. The specific surface area of ''sandwiched BP'' should be similar to that of a self-supporting BP membrane, as the PP support does not penetrate far into the BP active layer. The main benefits from the support were mechanical as reported in greater detail in the next section. The surface hydrophobicity of the composite was also reduced to ~90–100° compared to 120° for the pure BP.

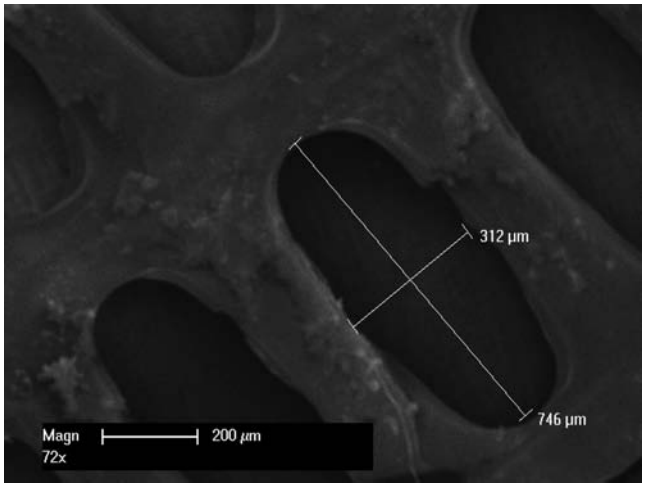

Fig. 2. Representative SEM image of the structure of the PP support.

The polymer infiltrated BP membranes exhibited a lower specific surface area of ~50 m^2/g, as well as a reduced hydrophobicity (~100° contact angle), compared to pure self-supporting membranes. Fig. 3 compares the surface of a self-supporting BP with a representative BP which was infiltrated with a 5% PS solution. The PS appears to partially coat the nanotubes reducing the membrane specific surface area. The reduced hydrophobicity is likely caused by the higher surface energy of the infiltrated polymer [16]. The characterization results are summarized in Table 1.

3.2. DCMD

3.2.1. Membrane permeability

Each composite CNT membrane was tested in a DCMD setup for a range of test conditions. The measured fluxes are plotted as a function of the water

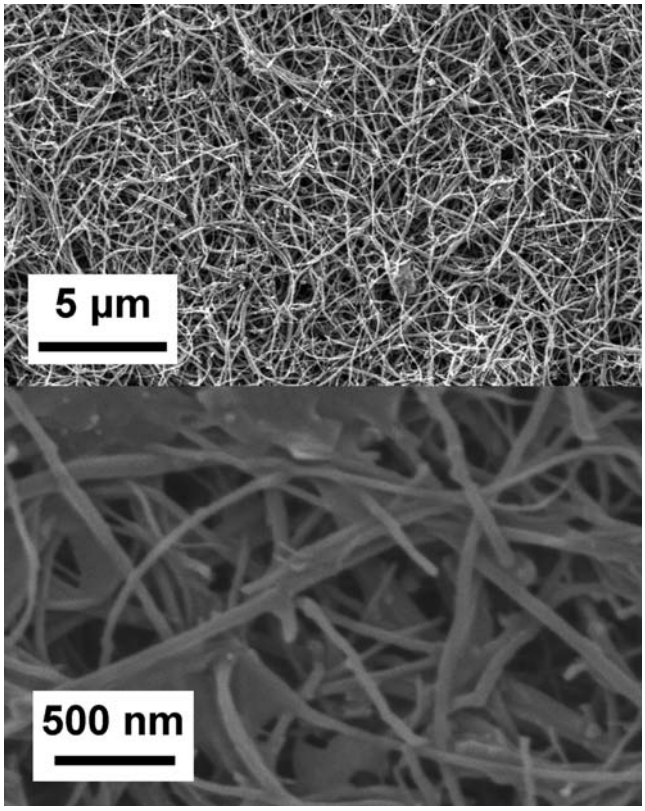

Fig. 3. Top: representative SEM image of the surface of a self-supporting BP membrane. Bottom: Representative SEM image of at the surface of a PS infiltrated composite BP membrane.

vapour partial pressure difference across the membrane (d*P*; Fig. 4). While self-supporting BP membranes presented fluxes of 6–10 kg/($m^2 \times h$), the composite membranes showed fluxes of up to 15 kg/$m^2 \times h$, for water partial pressure differences in the range of 5–45 kPa. As expected from theory [17], the flux increased linearly with water vapour partial pressure for each membrane. Permeances were calculated by taking the gradient of the best linear fit to the curves in Fig. 4. Then, permeabilities were calculated by multiplying the permeance value by the average a7ctive layer thickness.

Permeabilities between 1.6 and 3.3 $\times$ 10^{-12} kg/(m $\times$ s $\times$ Pa) were determined for the composite CNT membranes [9]. These values are up to four times that measured for the pure, self-supporting BP membranes, clearly demonstrating the benefit and potential of composite CNT membranes.

''Sandwiched BP'' membranes gave the best permeabilities of all the composite BP membranes, with a value of 3.3 $\times$ 10^{-12} kg/(m $\times$ s $\times$ Pa). Although the ''filtered sandwiched BP'' membrane is very similar in structure, its permeability is half that of the ''sandwiched BP'' membrane. This may result from a thicker CNT active layer. The ''filtered sandwich BP'' membranes were processed by filtering the CNTs through the PP support so that CNTs likely occupy partially the pores in the PP support while also forming a thin layer on top of it. However further characterisation work is needed to confirm this. The lower permeabilities measured for the ''polymer infiltrated BP'' membranes are consistent with the characterisation results, which indicated reduced porosity and specific surface area due to the polymer presence.

Even if composite BP membranes showed improved performances, those values still remained in average 0.5–2.5 times lower than the PTFE permeability. The best permeability measured for the CNT composite membranes was $\sim$60% that of the control PTFE membrane [9]. This is highly promising as PTFE membranes are amongst the best performing for MD. Several factors may contribute to the lower permeability measured for the composite CNT membranes compared to the PTFE control.

This may be firstly attributed to the BP membrane thermal conductivity, which is $\sim$10 times greater than that of PTFE. The thermal conductivity is an important property for the membrane distillation process as it determines the amount of heat transfer through the membrane thus influencing both temperature gradient and vapour pressure difference across the membrane.

Secondly, the structure and pore shape of PTFE membranes are distinctly different from the non-woven structure of self-supporting BP. The BP pores consist of an interconnected network of interstitial gaps between CNTs, while PTFE membranes pores are long and thin due to the stretching process used during their fabrication. The PTFE pores are also likely to be straighter, leading to a less tortuous path.

Furthermore, the average BP pore size is $\sim$10$-$15 times smaller than that for PTFE membranes. Theory on Knüdsen diffusion shows that the molar flux should be proportional to the radius of the pores, making this an important property affecting flux [18]. Pore size [19] and porosity [20] can be tuned in BP structures and work is currently underway to optimise these properties.

Finally membrane ageing, as discussed in the next section, may also contribute to the poorer permeability although further work is needed to confirm this.

3.2.2. Lifespan and salt rejection

The composite BP membranes exhibited improved salt rejection and lifespan compared with self-

Table 1
Properties of BPs membranes and DCMD results

	Thickness (mm)	Contact angle (°)	Porosity (%)	Pore size SEM imaging (nm)	Salt rejection (%)	BET (m^2/g)	Thermal conductivity (W/m^2 K)	Lifespan* (h)	Permeability 10^{-12} kg (m s Pa)
PTFE 0.2 μm pores	~200	130	70–75	200–400	99.9	21	0.25	—	5.51
Self-supporting BP	From 20	115–125	85–90	25–100	~90	197	2.3	3	0.83
Composite multi layer	~120–140	90–100	~62[+]	25–100	95.5	197[#]	—	39	3.31
Filtrated BP through support	~120–140	90–100	—	25–100	94.7	–	—	34	1.55[**]
Polymer infiltrated PS	~40–80	95–110	~55[+]	25–100	98.5	0	—	19	2.57
Polymer infiltrated PVDF	~40–80	95–110	—	25–100	96.5	—	—	16	1.89
Poly-propylene support	~100	95–110	—	25–100	—	—	—	—	–

[#]Mass of the PP support is included in this measurement.
[+]Porosity estimated from CNT ratio in composite.
[*]For composite and PTFE membranes, lifespan was defined as the time at which salt rejection dropped to 90%.
[**]Thickness of active layer taken as 40 μm.

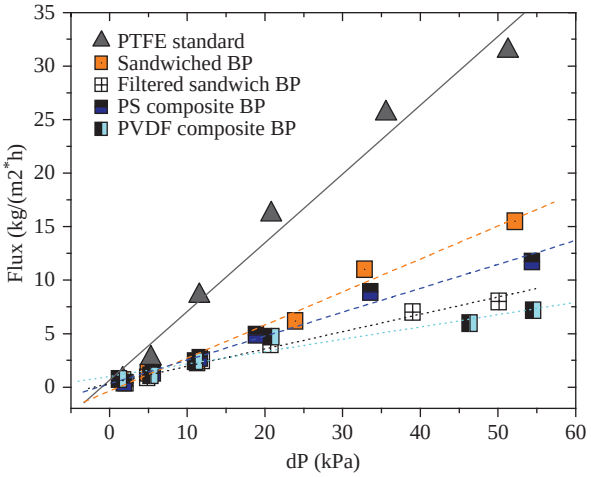

Fig. 4. Flux as a function of vapour pressure difference (d*P*) across the membrane. The vapour pressure difference was controlled by varying the hot side temperature (20°C; 35°C; 50°C; 65°C; 85°C; 95°C) while maintaining a constant cold side temperature of 5°C.

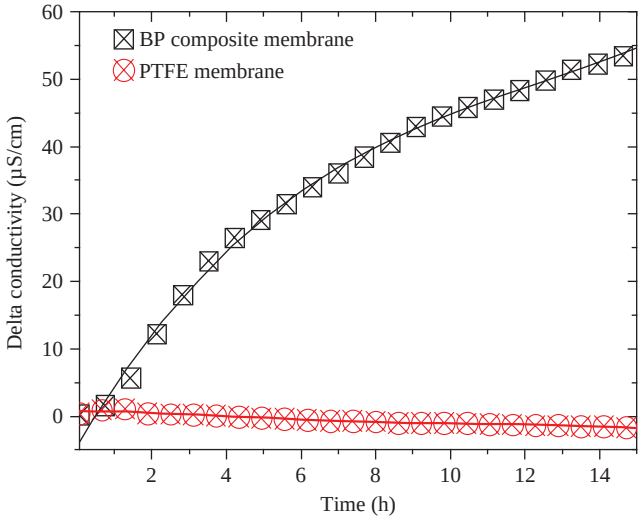

Fig. 5. Variation of permeate conductivity over time for a cracked BP composite membrane and a PTFE membrane.

supported structures. The lifespan was defined as the time taken for the salt rejection to drop below 90%. As shown in Fig. 5, a slow rise in permeate conductivity and hence a reduced salt rejection, is observed over time for most of the tested BP membranes and is related to membrane ageing as discussed in greater detail below. The best lifetime of 39 h was recorded for the ''sandwiched BP'' composite membranes and was 13 times higher than that for self-supporting BP membranes. Most of the composite BP membranes lasted for over 25 h, whereas all of the self-supporting membranes cracked within 3 h of continuous testing. This improvement is likely due to the extra reinforcement provided by the PP supports and infiltrated polymers.

The average salt rejection was increased from 90% for self-supporting BPs to 95% on average for the composite BP membranes (Table 1). This salt rejection was after each test and then average over the series. Salt rejection of ~98.5% were usually reached for the first tests but continuous testing progressively led to a decrease of salt rejection.

While testing self-supporting BPs, it was assumed that the high crack rate propagation was due to mechanical ageing due to the pulsation of the membrane in the module, thus reducing efficiency and lifespan of the membranes. The addition of the supports or of the infiltrated polymers led to increased stiffness and improved lifespan and more stable membranes. The surface of the sandwiched membranes was also more protected from flux variation or delamination due to the PP supports. It does however reduce their apparent porosity and direct surface of contact, thus diminishing the potential of the BPs.

Cross sections through the BP structures made by FIB milling clearly show the formation of cracks in some regions (Fig. 6). EDS analysis indicated the presence of sodium in these cracks, confirming that they form pathways for salty water to cross the membrane from the feed to permeate. Chlorine was not reported since the 5 keV accelerating voltage used was not enough to give a strong signal. However, crack formation in the composite CNT membranes was alleviated compared to the pure self-supporting structures, with longer lifespan and a slower rate of conductivity increase in the permeate.

The composite BP structures will be further optimised and other embedding methods and structures investigated to further extend membrane lifespan and improve their performance

4. Conclusion

In summary, a number of composite CNT membranes were processed from self-supporting BP membranes. We demonstrated that composite CNT membranes gave comparable flux and permeability to that of PTFE membranes and consistently performed better than their self-supporting BP counterparts. In the ''sandwiched BP'' structure, the PP supports improved the membrane lifespan by a factor 10, with membranes lasting for up to 40 h of continuous testing. The salt rejection efficiency of the composite structures was also improved with an average value of 95% for all

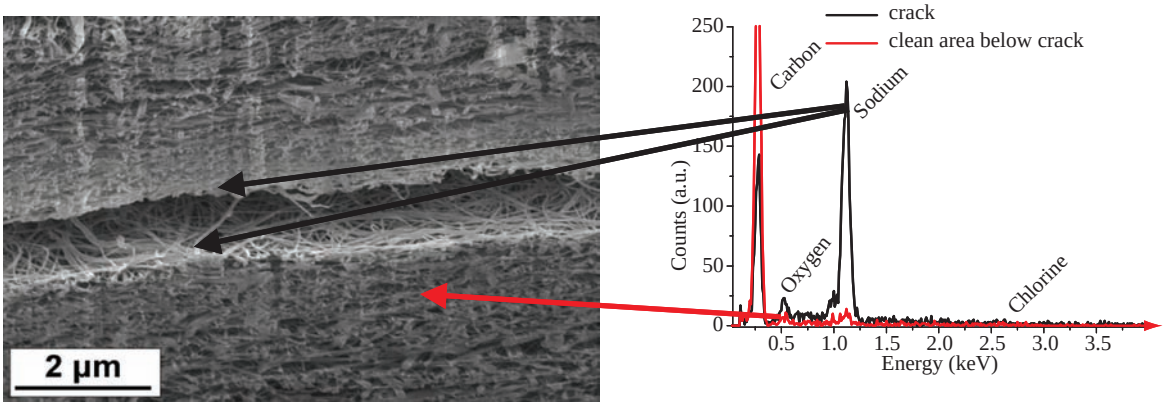

Fig. 6. Left: SEM image of a section milled with a FIB through a BP membrane after testing in the DCMD setup. Right: corresponding EDS analysis showing the presence of salts in the crack.

of the membranes while reaching 98.5% for some sandwiched structures.

The ''Sandwiched BP'' composite membranes were found to be the most efficient of the structures investigated in this work. However different geometries and material supports should be considered to fully optimize the membrane performance while taking best advantage of the CNTs properties.

Future work will concentrate on a number of other composite CNT membranes structures with the aim of improving their performance for DCMD. For example, larger pore size CNT based membranes may lead to improved flux and performance, while stiffer reinforcements or better connectivity between CNTs may resolve the ageing issue. Furthermore, different setups such as vacuum membrane distillation (VMD) may be tested if considered more suitable than DCMD for the BP structure and properties. Finally, work is also under way to fully characterize the BP thermal behaviour and identify how their heat diffusivity and heat conductivity affect the flux and the temperature gradient.

Acknowledgements

The authors would like to thank CSIRO Material Science and Engineering (CMSE) and the Institute for Sustainability and Innovation at Victoria University for financial support. We highly appreciated Dr. Stephen Hawkins and Chi Huynh nanotube quality (CMSE). Ludovic Dumée is also grateful to the Membrane Society of Australasia (MSA) – Millipore award which he received to attend AMS-5, Kobe, Japan. He was also deeply honoured to be granted the MSA-AMS-5 award for the best student presentation while presenting at the AMS-5 conference.

References

[1] S. Iijima, Helical microtubules of graphitic carbon, Nature, 354 (6348) (1991) 56–58.
[2] F. Peng, C. Hu and Z. Jiang, Novel ploy(vinyl alcohol)/carbon nanotube hybrid membranes for pervaporation separation of benzene/cyclohexane mixtures, J. Membr. Sci., 297(1–2) (2007) 236–242.
[3] F. Fornasiero, H.G. Park, J.K. Holt, M. Stadermann, C.P. Grigoropoulos, A. Noy and O. Bakajin, Ion exclusion by sub-2-nm carbon nanotube pores, Proc. Natl. Acad. Sci. USA, 105(45) (2008) 17250–17255.
[4] B.J. Hinds, N. Chopra, T. Rantell, R. Andrews, V. Gavalas and L.G. Bachas, Aligned multiwalled carbon nanotube membranes, Science, 303(5654) (2004) 62–65.
[5] A. Srivastava, O.N. Srivastava, S. Talapatra, R. Vajtai and P.M. Ajayan, Carbon nanotube filters, Nat. Mater., 3(9) (2004) 610–614.
[6] K.W. Lawson and D.R. Lloyd, Membrane distillation. II. Direct contact MD, J. Membr. Sci., 120(1) (1996) 123–133.
[7] R.W. Schofield, A.G. Fane, C.J.D. Fell and R. Macoun, Factors affecting flux in membrane distillation, Desalination, 77(1–3) (1990) 279–294.
[8] M. Gryta, M. Tomaszewska and K. Karakulski, Wastewater treatment by membrane distillation, Desalination, 198(1–3) (2006) 67–73.
[9] L. Dumée, K. Sears, J. Schütz, N. Finn, M. Duke and S. Gray, Characterization and evaluation of carbon nanotube bucky-paper membranes for direct contact membrane distillation, J. Membr. Sci., 2010, In press.
[10] R. Smajda, A. Kukovecz, Z. Konya and I. Kiricsi, Structure and gas permeability of multi-wall carbon nanotube buckypapers, Carbon, 45(6) (2007) 1176–1184.
[11] J. Wang, S.B. Hocevar and B. Ogorevc, Carbon nanotube-modified glassy carbon electrode for adsorptive stripping voltammetric detection of ultratrace levels of 2,4,6-trinitrotoluene, Electrochem. Commun., 6(2) (2004) 176–179.
[12] C. Huynh and S. Hawkins, Understanding the synthesis of directly spinnable carbon nanotube forests, Carbon, 48(4): P. 1105–1115.
[13] K. Smolders and A.C.M. Franken, Terminology for membrane distillation, Desalination, 72(3) (1989) 249–262.
[14] S.M. Cooper, H.F. Chuang, M. Cinke, B.A. Cruden and M. Meyyappan, Gas permeability of a buckypaper membrane, Nano Lett., 3(2) (2003) 189–192.
[15] S. Nuriel, L. Liu, A.H. Barber and H.D. Wagner, Direct measurement of multiwall nanotube surface tension, Chem. Phys. Lett., 404(4–6) (2005) 263–266.

[16] D.P. Instruments, Solid surface energy data (SFE) for common polymers.2007; Available from: http://www.surface-tension.de/solid-surface-energy.htm.
[17] M.S. El-Bourawi, Z. Ding, R. Ma and M. Khayet, A framework for better understanding membrane distillation separation process, J. Membr. Sci., 285(1–2) (2006) 4–29.
[18] A. Burgoyne and M.M. Vahdati, Direct contact membrane distillation, Sep. Sci. Technol., 35(8) (2000) 1257–1284.
[19] L. Dumée, K. Sears, J. Schütz, N. Finn, M. Duke and S. Gray. Design and Characterisation of Carbon Nanotube Bucky-Paper Membranes for Membrane Distillation in ICOM08. 2008, Honolulu, Hawaii, USA.
[20] R.K. Das, B. Liu, J.R. Reynolds and A.G. Rinzler, Engineered macroporosity in single-wall carbon nanotube films, Nano Lett., 9(2) (2009) 677–683.